Ageing and memory phenomena in magnetic and transport properties of vortex matter

2001 J. Phys. A: Math. Gen. 34 8425

(http://iopscience.iop.org/0305-4470/34/41/303)

INSTITUTE OF PHYSICS PUBLISHING JOURNAL OF PHYSICS A: MATHEMATICAL AND GENERAL

J. Phys. A: Math. Gen. **34** (2001) 8425–8443 PII: S0305-4470(01)26768-7

Ageing and memory phenomena in magnetic and transport properties of vortex matter

Mario Nicodemi[1,2] **and Henrik Jeldtoft Jensen**[1]

[1] Department of Mathematics, Imperial College, 180 Queen's Gate, London SW7 2BZ, UK
[2] Universitá di Napoli 'Federico II', Dip. Scienze Fisiche, INFM and INFN, Via Cintia, 80126 Napoli, Italy

E-mail: m.nicodemi@ic.ac.uk and h.jensen@ic.ac.uk

Received 5 July 2001
Published 5 October 2001
Online at stacks.iop.org/JPhysA/34/8425

Abstract

There is mounting experimental evidence that strong off-equilibrium phenomena, such as 'memory' or 'ageing' effects, play a crucial role in the physics of vortices in type II superconductors. In the framework of a recently introduced schematic vortex model, we describe the out-of-equilibrium properties of vortex matter. We develop a unified description of 'memory' phenomena in magnetic and transport properties, such as magnetization *loops* and their 'anomalous' *second peak*, logarithmic *creep*, 'anomalous' *finite creep rate* for $T \to 0$, *'memory'* and *'irreversibility'* of I–V characteristics, *time-dependent* critical currents, *'rejuvenation'* and *'ageing'* of the system response.

PACS numbers: 74.24.-q, 74.60.-w, 75.10.Nr

(Some figures in this article are in colour only in the electronic version)

1. Introduction

The properties of vortex dynamics in type II superconductors crucially affect the overall system behaviour and have, thus, relevant effects in technological applications [1–4]. In particular, in the last few years it has been discovered that vortex matter exhibits important, even dominant, history-dependent phenomena in magnetic and transport properties, such as memory and hysteresis in magnetization curves along with irreversibility and ageing in I–V characteristics (see [3, 4, 29, 31–39, 42, 44, 57, 58] and references therein). These phenomena are markedly *out-of-equilibrium* effects and, here, we discuss their features as they emerge from the off-equilibrium dynamics of vortex matter (see [1, 6–9]).

The above experimental findings have interesting analogies with 'memory' and 'ageing' effects observed in other glass formers, such as polymers, supercooled liquids or random

magnets [5, 6]. Interestingly, 'glassy' dynamics have important universal structural properties [5, 6]. Off-equilibrium features arise when typical experimental probing times get very short compared with the system long (often inaccessibly long) intrinsic relaxation time scales. These can become huge at low temperatures or high densities, where a true equilibrium glass phase transition in some cases can be also found. Such glass transitions are called 'ideal' [5] because, as just stated, equilibrium might be hardly approached. In fact, the notion of 'glassy phases' has been repeatedly used in relation to new *equilibrium* phases of vortex matter [1, 10–13]. We are concerned here, however, with the general properties of *off-equilibrium dynamics* of vortices, not with their equilibrium transitions. (Note that in several cases the 'ideal' transition is found at zero temperature, but the systems have apparent 'glassy' dynamics (see examples in [6].).

We consider a schematic model [14] that contains the essential degrees of freedom of a vortex system and is simple enough to allow a complete understanding of its off-equilibrium dynamics in the same perspective successfully used for other glassy systems [5,6]. The model (a coarse-grained [15, 16] system of repulsive particles wandering in a pinning landscape in the presence of a thermal bath and an external drive) describes several phenomena of vortex physics, ranging from a *re-entrant phase diagram* in the (B, T) (field–temperature) plane, to the anomalous *'second peak'* in magnetization loops (the 'fishtail'), *logarithmic creep* and *'ageing'* of magnetic relaxation, the *finite creep rates* for $T \to 0$ (without use of 'quantum effects'), *'memory'* and *history*-dependent behaviours in vortex flow and in I–V characteristics, and many others [14].

We describe here the properties of such a model and depict a unified picture of creep and transport measurements. In particular, the system dynamics can be described by identifying its important time scales and their dependence on temperature, magnetic field and applied electrical current. We also suggest new experiments that will help to clarify the nature of glassy aspects in superconductors.

In the next section we introduce the model [14] and in sections 3 and 4 we systematically compare its behaviours with experiments on magnetic and transport properties. Finally, in section 5 we give an overview of our scenario of off-equilibrium phenomena in vortex matter.

2. The ROM model

Vortices in type II superconductors are described by the Ginzburg–Landau equations. The typical high vortex densities and long interaction range imply that the vortex system is strongly interacting. In brief, this makes the theoretical description of its equilibrium and, even worse, dynamical properties highly non-trivial [1, 3].

An appealing and much used approximation for the *microscopic* vortex dynamics is based on molecular dynamics (MD) simulations (see, for instance, [17–20]). However, even this simplified approach is hardly feasible to explore the physics of the long time and space scales, and the low-temperature and high-density region where glassy features substantially appear [20]. Alternatively, it has been proposed to use schematic discrete time and space models [22] to study vortex properties.

More generally, to describe the relevant degrees of freedom of the vortex system one can introduce useful *coarse graining* methods, successfully applied to deal with many other multi-scale problems (such as magnetism or crystals defects, see [23]). For clarity, let us consider the simple case of a system of straight parallel vortex lines, corresponding to a magnetic field B along the z-axis, where vortices interact through a two-body potential [2]:

$$A(r) = \frac{\phi_0^2}{2\pi\lambda'^2}\left[K_0(r/\lambda') - K_0(r/\xi')\right] \tag{1}$$

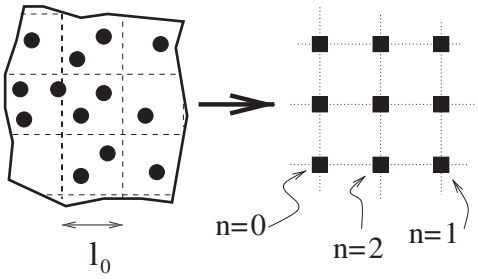

Figure 1. Schematic illustration of the procedure introduced to define the ROM lattice model. The original vortex system (left), coarse grained in 'cells' of size l_0, is mapped into a lattice field model (right).

K_0 being the MacDonald function, and ξ and λ the correlation and penetration lengths ($\xi' = c\xi/\sqrt{2}$, $\lambda' = c\lambda$, $c = (1 - B/B_{c2})^{-1/2}$, with B_{c2} the upper critical field). A simple application of the above methods in the present case, proposed in [14, 16], consists in coarse graining the vortex system in the xy-plane by introducing a square grid of lattice spacing, l_0, of the order of the London length, λ (see figure 1). (Note that for $l_0 \to \xi$ one recovers the original system dealt within MD.)

By this procedure, the original vortex system is mapped into a lattice model characterized by a classical field, n_i, representing the number of vortices on the ith coarse-grained cell (see figure 1). The presence in superconductors of an upper critical field, B_{c2}, implies that n_i must be an integer number smaller than $N_{c2} = B_{c2}l_0^2/\phi_0$ [14] (here $\phi_0 = hc/2e$ is the flux quantum, c the light speed, h the Planck constant and e the electron charge). The Hamiltonian of the coarse-grained model is [14]

$$\mathcal{H} = \tfrac{1}{2}\sum_{ij} n_i A_{ij} n_j - \tfrac{1}{2}\sum_i A_{ii}|n_i| - \sum_i A_i^p |n_i|. \tag{2}$$

The first two terms of $\mathcal{H}$ describe the repulsion between the vortices and their self-energy, and the last the interaction with a random pinning background. For the sake of simplicity, since $l_0 \sim \lambda$, we can consider the simplest version of $\mathcal{H}$: we choose $A_{ii} = A_0 = 1$; $A_{ij} = A_1 < A_0$ if i and j are nearest neighbours; $A_{ij} = 0$ otherwise; the random pinning is taken to be delta-distributed $P(A^p) = (1-p)\delta(A^p) + p\delta(A^p - A_0^p)$, where p is the fraction of sites with pinning amplitude A_0^p (see[1]). We express all energy scales in units of A_0 and, in particular, consider the important ratio $\kappa^* = A_1/A_0$. The existence of two possible orientations of the vortices can be taken into account by giving the particles, n_i, a 'charge' $s_i = \pm 1$ [1, 2]. Neighbouring particles with opposite 'charge' annihilate. The external applied field controls the overall system 'charge density' and thus a chemical potential term $-\mu \sum_i s_i n_i$ must be added to the Hamiltonian in equation (2) (where n_i is replaced by $s_i n_i$).

A standard mean field replica theory [14] allows us to evaluate the equilibrium phase diagram in the field–temperature plane of the above Hamiltonian, as shown in figure 2. In the absence of disorder it has, at low temperatures, a re-entrant order–disorder transition in agreement with predictions [1] and experiments on vortices in superconductors (see [1, 3, 4] or, for instance, data on 2H–$NbSe_2$ superconductors from [29]). For moderate values of the pinning energy ($A_0^p \leqslant A_1$), a second-order transition still takes place, which at sufficiently strong pinning is expected to become a 'glassy' transition, as is seen in random field Ising models [27]. The extension of the low-T phase shrinks by increasing A_0^p (i.e. the highest critical temperature, T_m^*, decreases) and the higher is κ^* the smaller the re-entrant region (facts in agreement with experiments: see, for instance, [3, 4, 28, 29]). The above phase diagram can help to compare experimental and model temperature/field scales.

[1] Here $A_0^p = 0.3A_0$, $N_{c2} = 27$, $p = 1/2$ and, if not differently stated, $A_1 = 0.28A_0$ (the $\mathcal{H}$ parameters can be related to the real material parameters [14]). $L = 32$, but the results are checked up to $L = 128$.

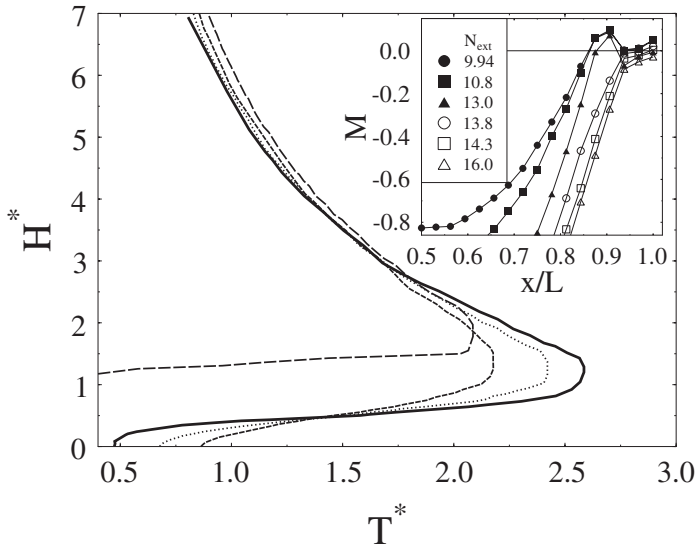

Figure 2. Mean field phase diagram of the ROM model in the plane (H^*, T^*) ($T^* = T/A_1$ and $H^* = \mu/k_B T$ are the dimensionless temperature and chemical potential of the applied field), for $\kappa^* = 10$ and $A_0^p = 0.0; 0.5; 0.75$ (results: full, dotted and dashed curves) and $\kappa^* = 3.3$ and $A_0^p = 0.0$ (long dashed curve). Inset: the magnetization Bean profile, $M(x)$, as a function of the transversal spatial coordinate x/L (L is the system linear size), for the shown values $N_{\rm ext}$, in the 2D ROM model (here $T = 0.3$, and the sweep rate of the external field is $\gamma = 1.1 \times 10^{-3}$). Notice the change in shapes when $N_{\rm ext}$ crosses $N_{\rm sp} \simeq 13.5$ (filled versus empty symbols).

We now go beyond mean field theory and discuss the dynamics of the model. First we consider the case where the external current is absent, i.e. there is no Lorentz drive on vortices. The simplest consistent approach to simulate the system relaxation at non-zero temperatures is a Monte Carlo Kawasaki dynamics [24], i.e. a dynamics in which particles can diffuse around coupled to the thermal bath and subject to their interaction potential landscape of equation (2). This is a very standard approach in computer simulations of dynamical processes in complex fluids [24]. In particular, we consider a system at a temperature T on a square lattice of size L (see footnote 3) periodic in the y-direction. Its two edges parallel to the y-axis are in contact with a vortex reservoir, i.e. an external magnetic field, of density $N_{\rm ext}$. Particles can enter and leave the system only through the reservoir.

The above model, called ROM (restricted occupancy model), is described in detail in [14]. It is extremely schematic, thus also fully tractable and, interestingly, it is able to describe many of the experimental observations on magnetic and transport properties of vortex physics.

3. The magnetization

The simplest quantity to characterize the vortices system is the magnetization, which we now consider. In this section we will draw a picture of time-dependent magnetic features such as magnetization *loops*, their *second peak*, *'ageing'* creep, as well as phenomena like the *finite creep rate*, $S_a > 0$, found when $T \to 0$.

The system is prepared by zero-field cooling at a given T and then increasing the external field, $N_{\rm ext}$, with a constant rate, γ. During the ramp of $N_{\rm ext}$ we record the magnetization

$$M(t) = N_{\rm in}(t) - N_{\rm ext}(t). \tag{3}$$

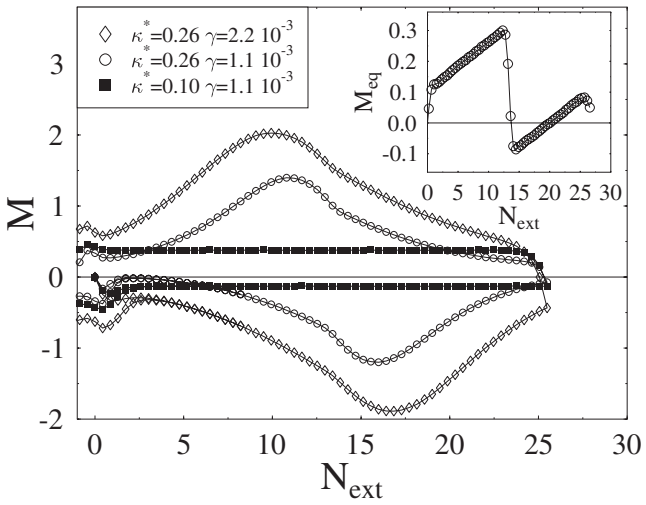

Figure 3. The magnetization, M, as a function of the applied field density, $N_{\rm ext}$, in the ROM model at $T = 0.3$ for the shown sweep rates γ and material parameters $\kappa^* = A_1/A_0$. Notice the appearance of a 'second magnetization peak' when κ^* is larger than a critical threshold $k_c^* \simeq 0.25$. Inset: the equilibrium value of M (i.e. when the field ramp rate $\gamma \to 0$) at $T = 0.3$ ($\kappa^* = 0.26$) shows an apparent first-order phase transition associated to the second magnetization peak.

Here $N_{\rm in} = \sum_i n_i/L^d$ and the Monte Carlo time, t, is measured in units of complete Monte Carlo lattice sweeps.

3.1. Magnetization loops

At low temperatures pronounced hysteretic magnetization loops are seen when M is plotted as a function of $N_{\rm ext}$ (see figure 3). Furthermore, when the parameter $\kappa^* = A_1/A_0$ (κ^* can be directly related to the Ginzburg–Landau parameter $\kappa = \lambda/\xi$ [14]) is above a critical threshold $k_c^* \simeq 0.25$, a definite *second peak* (the so-called experimental 'fish-tail') appears in M. Very similar magnetization data are observed in a number of different superconductors from intermediate to high κ values (see, for instance, [3, 4, 28–36, 44, 46] and references therein).

The actual shape of loops depends on the system parameters (and its size). In particular, the sweep rate of the external field, γ, is very important, as shown in figure 3. As soon as the inverse of the sweep rate is smaller than the system characteristic relaxation time (see below) strong hysteresis effects are present. Although the second peak does depend on the dynamics through γ, in the ROM model it is related to a new phase transition: in the $\gamma \to 0$ limit (i.e. when the external field is ramped quasi-statically) its location, $N_{\rm sp} = 13.5$, is associated with a sharp jump in $M_{\rm eq} \equiv \lim_{\gamma\to 0} M(\gamma)$ (see inset of figure 3). These findings are consistent with experiments (for instance, see [29–35, 39, 40, 44, 45]) and to some extents reconcile previously proposed opposite descriptions ('static' versus 'dynamic').

3.2. History-dependent relaxation: 'ageing' creep

The presence, at low temperature, of sweep-rate-dependent hysteretic cycles, slowly relaxing magnetization, and similar effects indicate that our system, on the observed time scales, is not at equilibrium. We turn, therefore, to the theoretical description of the system dynamics by investigation of two-times correlation functions. At a given working value of the applied

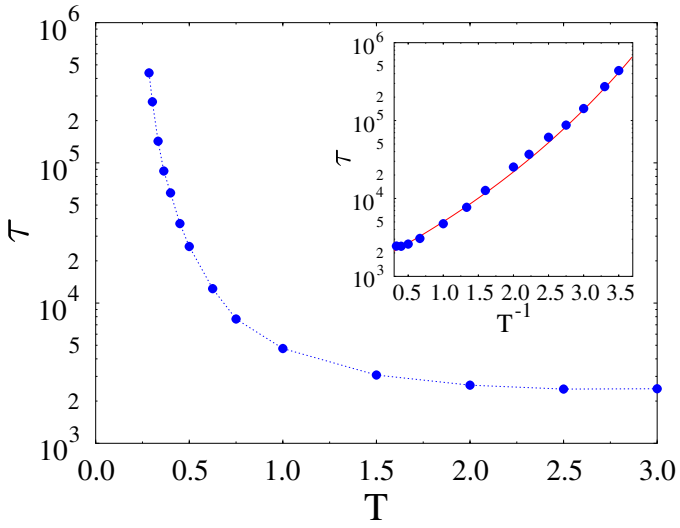

Figure 4. The system equilibration time, τ, from equation (5), grows enormously with decreasing temperature T (here $N_{\rm ext} = 10$). Below the crossover temperature $T_g \sim 0.25$, τ is larger than the observation window. Inset: close to T_g, τ plotted as a function of $1/T$ approximately shows a VTF behaviour, the continuous curve (see equation (6)).

field, we now also record the magnetic correlation function, $C(t, t_w)$ (with $t > t_w$), which gives richer information than $M(t)$ (since the general dynamical features of C and M are very similar, for clarity here we mainly discuss C):

$$C(t, t_w) = \langle [M(t) - M(t_w)]^2 \rangle. \tag{4}$$

At not too low temperatures, for instance at $T = 1.0$ (see figure 2 for a comparison of such a T value with experimental scales), the system creep is characterized by finite relaxation times and no 'ageing' is seen: $C(t, t_w)$ is a function of $t - t_w$. At long times, $C(t, t_w)$ is well fitted by the so-called Kohlrausch–Williams–Watts (KWW) law [14]:

$$C(t, t_w) \simeq C_\infty \left\{ 1 - \mathrm{e}^{-[(t-t_w)/\tau]^\beta} \right\}. \tag{5}$$

Equation (5) defines the characteristic time scale of magnetic relaxation, τ. This is a crucial quantity to be considered when dealing with dynamical aspects of magnetization. The Kohlrausch exponent, β, and τ strongly depend on T (a fact to be discussed below, see figure 4) and on the applied field $N_{\rm ext}$ [14]. The pre-asymptotic dynamics (i.e. $t - t_w \ll \tau$) is also interesting and characterized by various regimes. In particular, for not too short times, a power law is observed over several decades.

The scenario described for $T = 1.0$ is found in a broad region at low temperatures. However, around $T = 0.5$, a steep increase of τ is found (see figure 4). For instance at $N_{\rm ext} = 10$, for temperatures below $T_g \simeq 0.25$, the characteristic time gets larger than our recording window and the system definitely loses contact with equilibrium. The crossover temperature, $T_g(N_{\rm ext})$ (which may be a function of γ) has a physical meaning similar to the so-called phenomenological glass transition point in supercooled liquids [5]. The presence of an underlying 'ideal' glass transition point, $T_c(N_{\rm ext})$, is often located by some fit of the high-T data of τ (see inset of figure 4), such as a Vogel–Tamman–Fulcher (VTF) (or a power) law:

$$\tau = \tau_0 \exp\left(\frac{E_0}{T - T_c} \right). \tag{6}$$

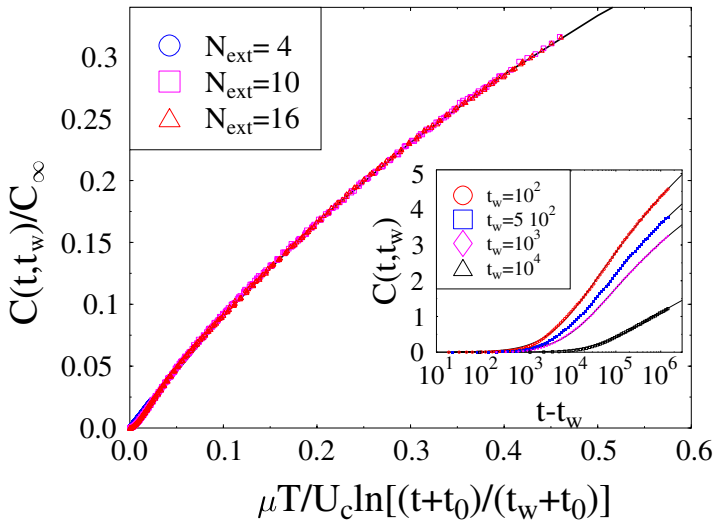

Figure 5. Inset: logarithmic time relaxation of the two-times correlation function, $C(t, t_w)$, as a function of $t - t_w$ for the shown values of t_w. Data are recorded at $T = 0.1$ (i.e. below T_g) and $N_{\rm ext} = 16$. The continuous curves are logarithmic fits from equation (7). Main frame: off-equilibrium dynamical scaling. The relaxation data of $C(t, t_w)$ from the inset and those recorded at $N_{\rm ext} = 4$, 10, 16 for each of the shown t_w are superimposed on the same master function. The asymptotic scaling is $C(t, t_w) \sim \mathcal{S}(t/t_w)$.

Our data in 2D are consistent with $T_c = 0$. Interestingly, the VTF behaviour found here is in agreement with results from MD simulations of more realistic London–Langevin models [14,17–20]. In particular, the analogies with 'window glasses' have been also outlined in the first reference of [20]. A VTF behaviour has been already experimentally observed in measures on samples resistivity (see [21]).

Since below T_g relaxation times are huge, one might expect that the motion of the particles essentially stops. Instead, as shown below, the off-equilibrium dynamics has remarkably rich 'ageing' properties. In the inset of figure 5 we show that $C(t, t_w)$, at $T = 0.1$, exhibits strong 'ageing': C depends on both times *t and t_w*; in particular, its evolution (see inset of figure 5) is slower the older is the 'age' t_w ('stiffening'). In the entire low-T region ($T < T_g$), after a short initial power law behaviour, $C(t, t_w)$ can be well fitted by a generalization of a known interpolation formula, often experimentally used [1, 3], which now depends on the *waiting time*, t_w:

$$C(t, t_w) \simeq C_\infty \left\{ 1 - \left[1 + \overline{u} \ln \left(\frac{t + t_0}{t_w + t_0} \right) \right]^{-1/\mu} \right\} \tag{7}$$

where the exponent $\mu = 1$ and C_∞, $\overline{u}$ and t_0 are T and $N_{\rm ext}$ dependent parameters. Equation (7) (in agreement with the general scenario of [41]) implies the presence of *scaling properties* of purely dynamical origin (see figure 5): for times large enough (but smaller than the equilibration time), C is a universal function of the ratio t/t_w: $C(t, t_w) \sim \mathcal{S}(t/t_w)$.

In experiments about vortex creep in superconductors a crossover is usually found from a low-T region with logarithmic creep to a high-T region with typically power law or stretched exponential relaxations (see for instance [43] and references in [3]). In particular, ageing in magnetic creep has been recently observed in BSCCO samples [42]. We also recall that the above phenomena are intriguingly common to many different systems ranging from polymers, to supercooled liquids [5], spin glasses [6, 54] and granular media [59].

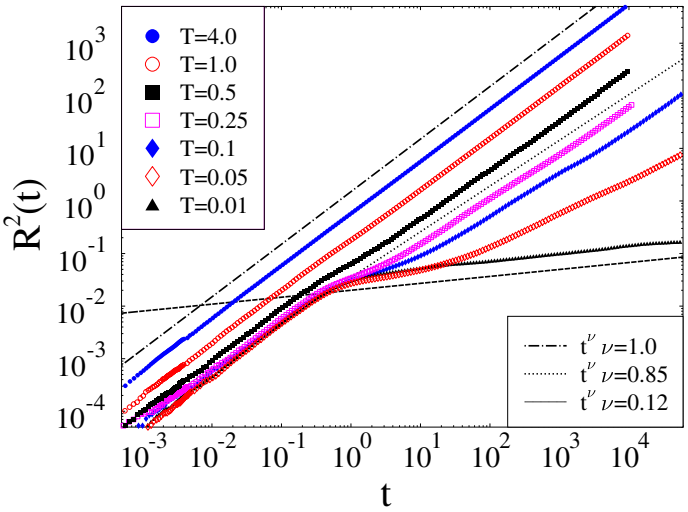

Figure 6. The vortex mean square displacement $R^2(t)$ at $N_{\rm ext} = 10$ for several temperatures. Below $T_g \sim 0.25$, $R^2(t)$ is strongly sub-diffusive: $R^2(t) \sim t^\nu$ with $\nu < 1$. Straight lines are guides for the eye.

3.3. Vortex mean square displacement

The microscopic origin of the above features in the system dynamics can be understood by considering the vortex mean square displacement, $R^2(t)$ (plotted in figure 6 for $N_{\rm ext} = 10$). At high enough T, $R^2(t)$ is linear in t (in agreement with experiments and MD simulations, see [47,48] and references therein), but at lower temperatures it shows a pronounced bending. Finally, below T_g, the process becomes strongly sub-diffusive:

$$R^2(t) \sim t^\nu \tag{8}$$

with $\nu \ll 1$. From this point of view, T_g is the location of a sort of structural arrest of the system, where particle displacement is dramatically suppressed. Each vortex is caged by other neighbouring vortices for long times. The system dynamics needs large-scale 'co-operative rearrangements' to relax [5]. Interestingly, a very similar scenario has been recorded in real superconducting samples (see for instance [44]).

3.4. The creep rate, S_a, for $T \to 0$

With the insight on the system dynamics obtained in the previous sections, we can now understand another intriguing experimental observation [49–52] about vortex matter: even at very low temperatures (where activated processes should be absent) magnetic relaxation does take place. This surprising phenomenon, previously interpreted in terms of 'quantum tunnelling' of vortices [1], is also found in the present purely 'classical' vortex model. More generally, we show here that a non-zero creep rate for $T \to 0$ is to be expected in systems 'ageing' in their off-equilibrium dynamics.

Experiments investigate the temperature dependence of the creep rate, S_a, (see figure 7), where

$$S_a = \left| \frac{\partial \ln(M)}{\partial \ln(t)} \right| \tag{9}$$

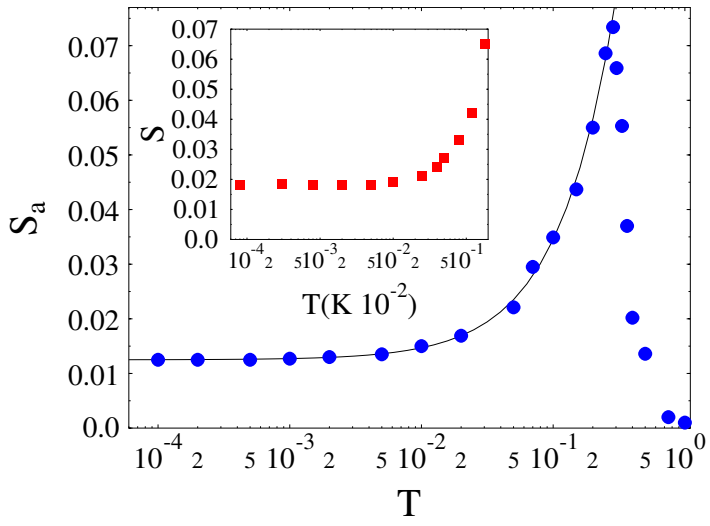

Figure 7. The creep rate, S_a, in the ROM model for $N_{\rm ext} = 10$ as a function of the temperature, T, in units of A_0 ($\kappa^* = 0.28$, $\gamma = 10^{-3}$). The superimposed curve is a linear fit. Inset: creep rate, S, in a BSCCO single crystal at 880 Oe (from Aupke *et al* [49]).

(S_a is, as usual, averaged in some given temporal window [3, 49–52]). When the temperature is extremely low the magnetization still logarithmically relaxes (see inset figure 8) and in both experiments and in our simulations S_a approaches a *finite* plateau, $S_a(0) > 0$, for $T \to 0$. In figure 7, we plot the creep rate, S_a, as a function of T. For comparison we present experimental data in BSCCO (from [50]) as inset (note that the values of S_a in our model and in real samples are very similar). In particular, we find that a linear fit of $S_a(T)$ in the low-T regime is very satisfactory (see figure 7):

$$S_a(T) = S_a^0 + \sigma T \tag{10}$$

where both S_a^0 and σ are functions of the applied field $N_{\rm ext}$. In the present model, as much as in experiments [3, 51], $S_a(T)$ is non-monotonic in T: at high T it starts decreasing (this is due to the fact that, for a given observation window, at higher T the system gets closer to equilibrium, see figure 4 and [14]).

By varying the applied field we find a range of values for S_a^0 very similar to experimental ones [49–52] and, in particular, S_a^0 seems to decrease on average by increasing the field $N_{\rm ext}$ (see figure 8). The overall behaviour can be roughly interpolated with a power law: $S_a^0(N_{\rm ext}) \simeq (N_{\rm ext}/N_0)^{-x}$, where, for $\kappa^* = 0.28$, $N_0 \simeq 0.01$ and $x \simeq 0.6$. As shown in figure 8, the presence of a small exponent, x, implies that sensible variations in S_a^0 can be seen only by changing $N_{\rm ext}$ by orders of magnitude. Note that in figure 8 the dips in the $S_a(0)$ versus $N_{\rm ext}$ data found at certain values of $N_{\rm ext}$ (namely around 3, 13, and 20) are statistically significant. They are located respectively close to the region of the low-field order–disorder transition (see figure 2), the second peak transition and the re-entrant high-field order–disorder transition.

In the slow off-equilibrium relaxation at very low temperatures no activation over barriers occurs and the system simply wanders in its very high-dimensional phase space through the few channels where no energy increase is required. We have already shown that at very low T, the system equilibration time, $\tau(T)$, diverges exponentially. In that region, the typical observation time windows, $t_{\rm obs}$, are such that $t_{\rm obs}/\tau \ll 1$, and the system is in the early stage

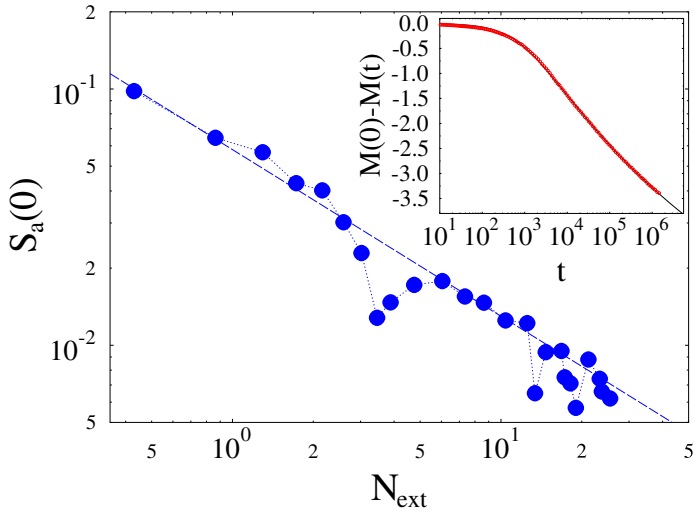

Figure 8. The $T \to 0$ limit of the creep rate, S_a, in the ROM model as a function of the applied field $N_{\rm ext}$ (for $T = 10^{-4}$ and $\gamma = 10^{-3}$). The superimposed dashed curve is a power law to guide the eye. Inset: the relaxation of the magnetization, $M(t)$, in the model for $N_{\rm ext} = 10$ and $T = 0.25$ as a function of time ($\gamma = 10^{-3}$). The continuous curve is the logarithmic fit of the text.

of its off-equilibrium relaxation from its initial state. This is schematically the origin of the flattening of S_a at very low T [14]. Notice that, in a system observed for an exponentially long time, i.e. for $t_{\rm obs}/\tau \gg 1$, the creep rate, S_a, would indeed go to zero.

Interestingly, our model in the limit $T \to 0$ along with a saturation of the creep rate, $S(T)$, also shows a saturation of dissipation related quantities. We show in figure 9 the differential resistivity, $\rho(T) = {\rm d}V/{\rm d}I$, measured for the same value of the model parameters used in the calculation of the creep rate $S(T)$ of figure 7 (the precise definition of V and I is postponed to the next section where we consider the I–V characteristics). The continuous curve superimposed to $\rho(T)$ in figure 9 corresponds to the linear fit $\rho(T) = \rho_0 + \sigma_\rho T$. These results clearly show a saturation in $\rho(T)$ at low T towards a finite value, in a way similar to the one recorded in $S(T)$.

The present scenario, where off-equilibrium phenomena dominate the anomalous low-T creep, is supported by the experimental discovery of 'ageing' in the system relaxation [29, 32, 34, 36, 42, 57, 58]. In fact, strong discrepancies are found between 'quantum creep theory' predictions [1] and the observed low-T relaxation in many compounds [14, 52, 53]. Interestingly, here a unified picture begins to emerge of magnetic and transport properties. This is discussed further in the next section.

4. The I–V characteristic

Vortex flow in driven type II superconductors also shows strong memory and history-dependent effects. Here, we outline the relations with magnetic properties and propose a scenario for a broad set of these kind of phenomena ranging from *'rejuvenation'* and *'stiffening'* of the system response, to *'memory'* and *'irreversibility'* in I–V characteristics. In relation to recent experimental results [57, 58], we discuss in particular the nature of 'memory' effects observed in the response of the system to an external drive, i.e. the I–V characteristic. Our model explains the peculiar form of such a 'memory' of vortex flow at finite T and other 'anomalous'

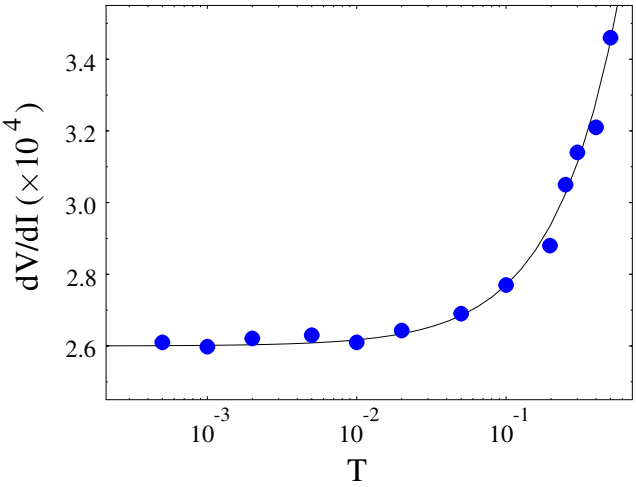

Figure 9. The differential resistivity, $\rho = \mathrm{d}V/\mathrm{d}I$, in the ROM model is plotted as a function of the temperature, T, for $N_{\mathrm{ext}} = 10$. The continuous superimposed curve is a linear fit. The saturation of $\rho(T)$ for $T \to 0$ well compares with the one of the magnetic creep rate, $S(T)$.

properties such as the time dependence of critical currents. The essential step is, again, to identify the relevant time scales in the dynamics.

The system is zero-field cooled and prepared by increasing N_{ext} at constant rate, γ, up to the working value (here, $N_{\mathrm{ext}} = 10$). Then we monitor the system relaxation after applying a drive, I (due to an external current which induces a Lorentz force on vortices), in the y-direction. As in similar driven lattice gases [25], the effect of the drive is simulated by introducing a bias in the Metropolis coupling of the system to the thermal bath: a particle can jump to a neighbouring site with a probability $\min\{1, \exp[-(\Delta\mathcal{H} - \epsilon I)/T]\}$. Here, $\Delta\mathcal{H}$ is the change in $\mathcal{H}$ after the jump and $\epsilon = \pm 1$ for a particle trying to hop along or opposite to the direction of the drive and $\epsilon = 0$ if orthogonal jumps occur. A drive I generates a voltage V [26]:

$$V(t) = \langle v_a(t) \rangle \tag{11}$$

where $v_a(t) = \overline{v}(t)$ is an average vortex 'velocity' at time t [14]. Here, $v(t) = \frac{1}{L}\sum_i v_i(t)$ is the instantaneous flow 'velocity', $v_i(t) = \pm 1$ if the vortex i at time t moves along or opposite to the direction of the drive I and $v_i = 0$ otherwise.

4.1. Memory effects in driven vortex flow

We analyse a striking manifestation of 'memory' observed in experiments where the drive is cyclically changed in the low-T region [58]. A drive I is applied to the system and, after a time t_1, abruptly changed to a new value I_1; finally, after waiting a time t_2, the previous I is restored and the system evolves for a further t_3 (see lower inset of figure 10). The measured $V(t)$ is shown in the main panel of figure 10 for $T = 0.1$. A first observation is that after the switch to I_1 the system seems to abruptly reinitiate its relaxation approximately as if it has always been at I_1 (see the caption of figure 10), a phenomenon known as *'rejuvenation'* in thermal cycling of spin glasses and other glassy systems [60]. The more surprising fact is, however, that for I_1 small enough (say $I_1 \ll I^*$, $I^* \sim \mathrm{O}(1)$ to be quantitatively defined below) when the value I of the drive is restored the voltage relaxation seems to restart from where it was at t_1, i.e. where it stopped before the switch to I_1 (see figure 10). Actually, if one 'cuts' the evolution during t_2

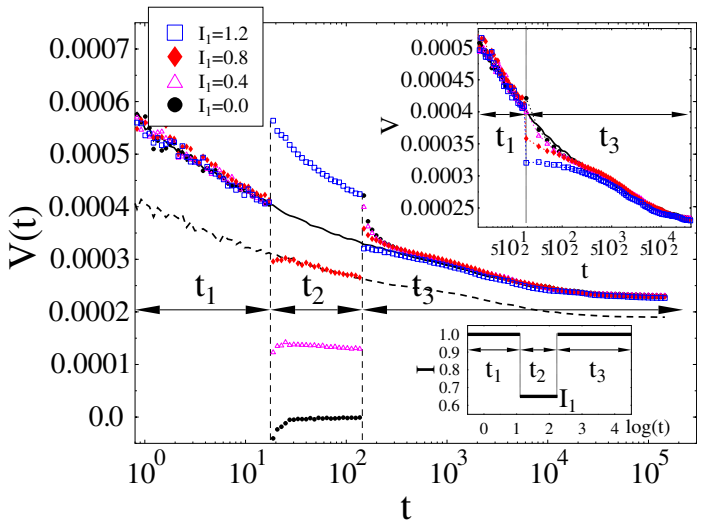

Figure 10. In the ROM model (at $T = 0.1$, $N_{\rm ext} = 10$) the voltage, $V(t)$, is plotted as a function of time for a drive $I = 1$ (see the continuous bold curve). As shown in the lower inset, after a time lag t_1, the drive is abruptly changed to I_1 for a time t_2 and finally it is set back to its previous value. When I is switched to I_1 (in the figure we plot data for the shown four different values of I_1) the system seems to *'rejuvenate'*: it suddenly restarts its relaxation along the path it would have had if $I = I_1$ at all times (consider the continuous and dashed bold curves, corresponding to $I = I_1 = 1$ and $I = I_1 = 0.8$, plotted for comparison). By restoring the drive to $I = 1$ after a time t_2, the system shows a strong form of 'memory': if t_2 and I_1 are small enough (see text) the relaxation of $V(t)$ restarts where it was at t_1. However, if t_2 and I_1 are too large, this is not the case, as shown in the upper inset. In this sense, the above is an *'imperfect memory'*.

and 'glues' together those during t_1 and t_3, an *almost* perfect matching is observed (see upper inset of figure 10). In particular, the matching is better the smaller I_1. What is happening during t_2 is that the system is trapped in some metastable states, but *not* completely frozen as shown by a small magnetic, as well as voltage, relaxation. These non-trivial 'memory' effects are experimentally found in vortex matter [58] and glassy systems [60]. We call them a form of *'imperfect memory'*, because they tend to disappear when the time spent at I_1 becomes too long or, equivalently (as explained below) when, for a given t_2, I_1 becomes too high, as shown in the upper inset of figure 10.

4.2. History-dependent I–V

We now turn to the time-dependent properties of the current–voltage characteristic. As in real experiments on vortex matter [58], we let the system undergo a current step of height I_0 for a time t_0 before starting to record the I–V by ramping I, as sketched in the inset of figure 11. Figure 11 shows (for $T = 0.1$) that the I–V depends on the waiting time t_0. The system response is 'ageing': the longer t_0, the smaller the response, a phenomenon known as *'stiffening'* in glass formers [5, 6, 60]. These effects are manifested in the violation of time translation invariance of two-times correlation functions, already discussed.

These simulations also reproduce the experimentally found time dependence of the critical current [58]. Usually, one defines an effective critical current, $I_c^{\rm eff}$, as the point where V becomes larger than a given threshold (say $V_{\rm thr} = 10^{-5}$ in our case): one then finds that $I_c^{\rm eff}$ is t_0 and I_0 dependent (like in experiments [58] $I_c^{\rm eff}$ is slowly increasing with t_0, see figure 11).

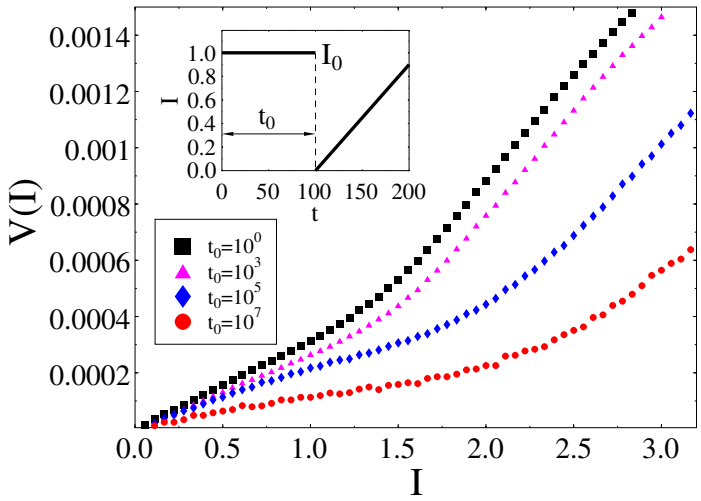

Figure 11. The I–V obtained at $T = 0.1$ by ramping I after keeping the system in presence of a drive $I_0 = 1$ for a time t_0 as shown in the inset. The response, V, is 'ageing' (i.e. depends on t_0) and, more specifically, *stiffening*: it is smaller the longer t_0.

It is interesting to consider another current cycling experiment which outlines the concurrent presence of irreversibility and memory effects (see figure 12). The I–V is measured by ramping I up to some value $I_{\max}$. Then I is ramped back to zero, but at a given value I_w the system is let to evolve for a long time t_w (in the main panel of figure 12, I_w is located by an upwards arrow; the two arrows correspond to two different values for I_w). Finally, I is ramped up again (see inset of figure 12). The resulting *irreversible* $V(I)$ is shown in figure 12. For $I > I_w$ the decreasing branch of the plot (empty circles) slightly deviates from the increasing one (filled circles), showing the appearance of *irreversibility*. This is even more apparent after t_w: for $I < I_w$ the two paths are clearly different. Interestingly, upon increasing I again (filled triangles), $V(I)$ does not match the first increasing branch, but the latest, the decreasing one: in this sense there is coexistence of memory and irreversibility. Also very interesting is that by repeating the cycle with a new I_w (squares), the system approximately follows the *same* branches. This non-reversible behaviour is also found in other glassy systems [60]. However, spin glasses, for instance, seem to show the presence of the so-called *chaos effects* [60, 61]. (This corresponds to the hypothesis that the free energy of metastable states vary chaotically with temperature, see for instance [61].) The chaos effect is absent in our system as it is also in other ordinary glass formers [6, 60]. This kind of interplay between irreversibility and memory can be checked experimentally in superconductors and thereby assess the present scenario.

4.3. Differential resistivity

In figure 13, we plot the I–V recorded after ramping I at $T = 1$ (filled squares) and $T = 0.1$ (open circles). The low-T I–V has the typical S shaped form experimentally found [3, 4, 55–58], but, interestingly, this is only an effect of short times of observation. The linear continuous functions in figure 13 are, in fact, the *asymptotic* I–V, i.e. those recorded after applying a drive I and measuring V in the long-time regime (for $t = 1.5 \times 10^5$ in figure 14). The same analysis applies to the differential resistivity, $\rho = \mathrm{d}V/\mathrm{d}I$, shown

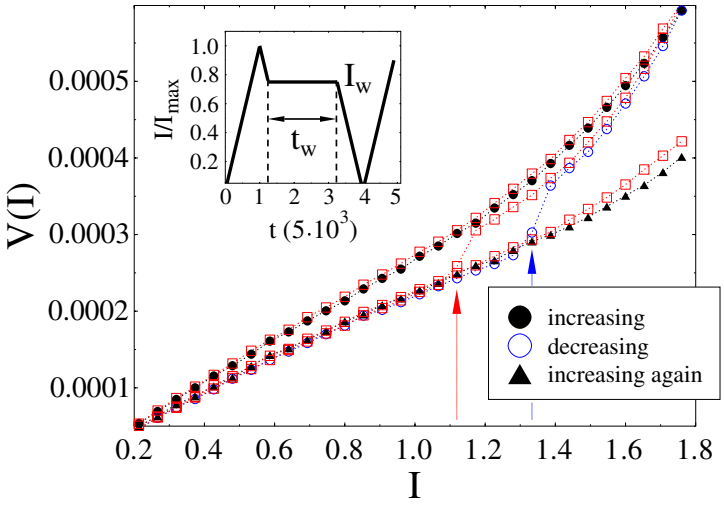

Figure 12. The I–V is measured at $T = 0.1$ during cycles of I (see also the inset): I is at first increased up to $I_{\max}$ (filled circles); along the descending branch of the cycle (empty circles), when $I = I_w$ (in the main panel the I_w, for two cycles, are located by the arrows) the drive is kept fixed for a time $t_w = 10^4$ and then the cycle restarted; finally, I is ramped up again (filled triangles). For $I > I_w$, the first increasing ramp and the decreasing one (resp. filled and empty circles) do not completely match, showing *irreversibility* in the I–V. After waiting t_w at I_w, a much larger separation is seen. However, by raising I again (filled triangles) a strong *memory* is observed: the system does not follow the first branch (filled circles), but the decreasing one (empty circles). Furthermore, in a cycle with a lower I_w (squares), the *same* branches are found.

in the inset of figure 13. One might also expect to see here some characteristic regimes (defined, for instance, by the values I_m, I_p of the inset of figure 13) in the 'short time' $\rho(I)$. They might be the off-stationarity, finite-temperature rests of crossovers between different plastic channel flow regimes typically found at $T = 0$, as discussed in [16–18, 48] and references therein (see also [63]). Here, the linear behaviour of the asymptotic I–V indeed shows that the crossovers in the 'short time' $\rho(I)$ tend to slowly disappear with time, thus they cannot correspond to transitions among different driven stationary phases [17–20, 57, 58, 63]. This conclusion holds despite the regular behaviour of I_m and I_p with T also experimentally seen (for instance I_p seems to rapidly grow with T). An intrinsic structure in ρ can possibly be observed at sufficiently lower currents and temperatures [63].

4.4. Voltage relaxation

The natural step to understand the above observations is the identification of the characteristic time scales of the driven dynamics, which in the present model can be well accomplished. This we now discuss. Upon applying a small drive, I, the system response, V, relaxes following a pattern with two very different parts: at first a rapidly changing nonlinear response is seen, later followed by a very slow decrease towards stationarity (see $V(t)$ in figure 14 for $T = 1$ and $I \in \{1, 2, 3\}$). For instance, for $I = 3$ in a time interval $\Delta t \simeq 2 \times 10^{-1}$, V leaps from about zero to $\Delta V_i \sim 2 \times 10^{-3}$, corresponding to a rate $r_i = |\Delta V_i / \Delta t| \sim 10^{-2}$. This is to be compared with the rate of the subsequent slow relaxation from, say, $t = 2 \times 10^{-1}$ to $t = 10^4$, $r_f \sim 10^{-7}$: r_i and r_f differ by five orders of magnitude.

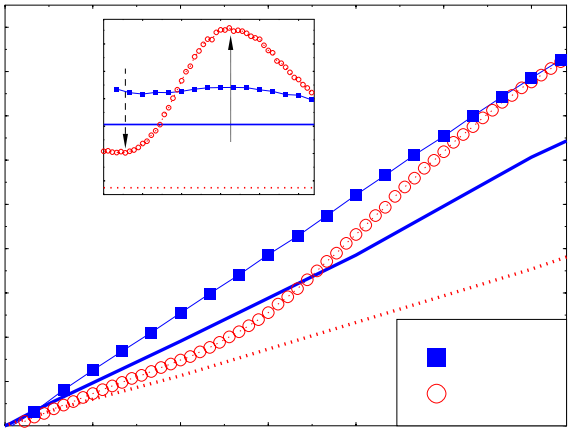

Figure 13. The I–V is recorded by ramping I for the shown T. The continuous and dotted curves (resp. $T = 1, 0.1$) are the *asymptotic* I–V, i.e. those where, for a given I, V is measured after waiting $t = 1.5 \times 10^5$ (see figure 14). Inset: the differential resistivity, $\rho = \mathrm{d}V/\mathrm{d}I$, for the same data of the main panel. The horizontal lines are from a linear fit to the *asymptotic* I–V. The characteristic values I_m and I_p roughly locate crossover points in the 'short time' ρ, which, however, disappear if $t \to \infty$.

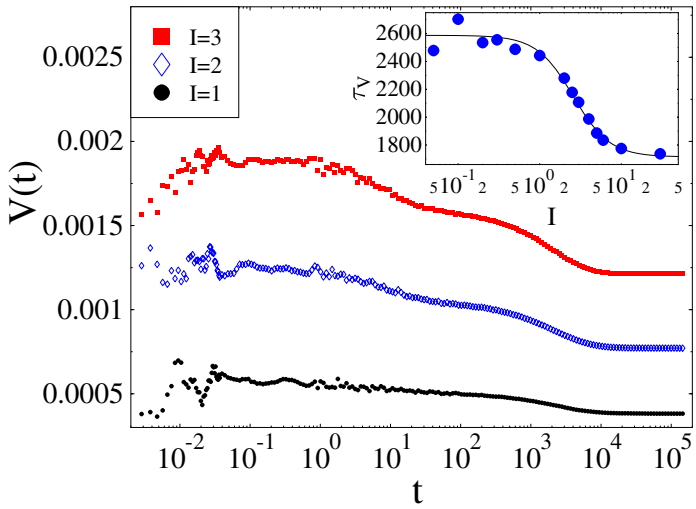

Figure 14. The time evolution of the response function, $V(t)$, for the shown values of the drive I (at $T = 1$ and $N_{\mathrm{ext}} = 10$). In the asymptotic regime $V(t)$ is well fitted with $V(t) \propto \exp[-(t/\tau_V)^{\beta}]$. Inset: the characteristic scale of relaxation, $\tau_V(I)$, as a function of I. For $I \to 0$, $\tau_V(I)$ seems to saturate to a *finite* value which implies that at $T = 1$ the critical current is zero, $I_c = 0$.

In agreement with experimental findings [57, 58, 62], the slow relaxation of $V(t)$ has a characteristic double-step structure, which asymptotically can be well fitted by stretched exponentials: $V(t) \propto \exp(-t/\tau_V)^{\beta}$. (At lower T inverse logarithmic relaxations are found [14].) The above long-time fit defines the characteristic asymptotic scale, τ_V, of relaxation under driving. The exponent β and τ_V are a function of I, T and N_{ext} (see inset

figure 14): in particular $\tau_V(I)$ decreases with I and seems to approach a *finite plateau* for $I < I^*$, with $I^* \simeq \mathrm{O}(1)$. In this sense, the presence of a drive I makes the approach to stationarity faster and has an effect similar to an increase in T.

The outlined properties of τ_V clearly explain the history-dependent effects in the experiments previously considered. For instance, the 'imperfect memory', discussed in figure 10, is caused by the presence of a long, but finite, scale τ_V in the problem: for a given I_1 the system seems to be frozen whenever observed on times scales smaller than $\tau_V(I_1)$. Thus, if t_2 is short enough ($t_2 < \tau_V(I_1)$) the system preserves a strong 'memory' of its state at t_1. The weakening of such a 'memory' found for higher currents I_1 in figure 10 is also a consequence of the strong decrease of $\tau_V(I)$ with I. The phenomenon of 'rejuvenation' (see figure 10) is, in turn, a consequence of the presence of the extremely fast first part of relaxation found in $V(t)$ upon applying a drive and of the above long-term memory. The existence of the slow part in the $V(t)$ relaxation also affects the 'stiffening' of the response in the I–V of figure 11, which is due to the non-stationarity of the vortex flow on scales smaller that τ_V. Actually, in figure 11, for a given I the value of V on the different curves corresponds to the system being probed at different stages of its non-stationary evolution. Finally, in brief, the fact that $\tau_V(I)$ is smaller at high currents, I, and larger at small I (and T), is responsible for the surprisingly concomitant effects of irreversibility and memory of figure 12.

The origin of these time-dependent properties of the driven flow, and in turn those of I–V, traces back to the concurrent vortex creep and reorganization of vortex domains. In fact, both with or without an external drive, the system evolves in the presence of a Bean-like profile (see inset of figure 2) which in turn relaxes. An important discovery is that the characteristic times scales of voltage and magnetic relaxation are approximately proportional [14]. This outlines that the non-stationary voltage relaxation is structurally related to the reorganization of vortices during the creep (a fact confirmed by recent experiments [36]).

5. Conclusions

In conclusion, we showed that the replica mean field theory and Monte Carlo simulations of a schematic statistical mechanics lattice model [14] for vortices in type II superconductors (a system of particles diffusing in a pinning landscape) offer a comprehensive framework of off-equilibrium magnetic and transport properties observed in vortex matter. Off-equilibrium phenomena in many respect are known to show strong 'universalities' [5, 6]. In fact, here we considered either a mean field or a two-dimensional version of the ROM model, which, interestingly, reproduces a very broad spectrum of experimental results. MD simulations of more realistic systems, when existing, seem to confirm the present scenario [14, 17–20], and, though very demanding in the low-T and high-field region, they can be an essential test for it.

We have seen that the model shows a re-entrant phase diagram in the field–temperature plane (B, T), analogous to what is observed in vortex matter. More specifically, we discussed the off-equilibrium, 'ageing', properties of magnetic creep. At low temperatures a crossover point is found, $T_g(N_{\mathrm{ext}})$, where the system relaxation times become exponentially large. They seem to diverge à la VTF at a lower temperature, $T_c(N_{\mathrm{ext}})$, where an 'ideal' glassy transition point can be located. Magnetic creep changes its structure around T_g: above T_g it shows power laws asymptotically followed by stretched exponential saturation; below T_g it is logarithmic. This corresponds to a change in microscopic vortex motion: from diffusive (above T_g) to strongly sub-diffusive [14]. We showed that in the low-temperature region the system is very far from equilibrium and its time correlation functions, no longer invariant under time translations, have interesting dynamical scaling properties analogous to those of other 'ageing' systems. The above 'off-equilibrium' scenario also explains the surprising experimental discovery of a

finite creep rate, $S_a > 0$, when $T \to 0$ (previously interpreted in terms of 'quantum tunnelling' of vortices [1]) in the same framework of our purely 'classical' model.

At not too high temperatures (but still well above T_g), magnetization loops are typically found when M is plotted as a function of the applied field, including a definite 'second peak' when the Ginzburg–Landau parameter is above a critical threshold. The 'second peak' is associated with a new phase transition in the system. This can be difficult to see in experiments because samples can be significantly out of equilibrium, as shown by the dependences of the loops on the external field sweep rate.

Vortex flow in driven type II superconductors also shows strong memory and history-dependent effects. We proposed a scenario for a broad set of these kind of phenomena ranging from 'rejuvenation' and 'stiffening' of the system voltage response, 'memory' and 'irreversibility' in I–V characteristics, to history-dependent critical currents. In particular, we have shown how creep and transport properties in driven media are related.

The emerging unifying scenario of magnetic and transport properties in vortex physics that we discussed has interesting relations with off-equilibrium phenomena in other glass formers and complex fluids such as random magnets and supercooled liquids.

Acknowledgments

HJJ is supported by the British EPSRC. MN acknowledges support from INFM-PRA(HOP) and INFM-PCI.

References

[1] Blatter G, Feigel'man M V, Geshkenbein V B, Larkin A I and Vinokur V M 1994 *Rev. Mod. Phys.* **66** 1125
[2] Brandt E H 1995 *Rep. Prog. Phys.* **58** 1465
[3] Yeshurun Y, Malozemoff A P and Shaulov A 1996 *Rev. Mod. Phys.* **68** 911
[4] Cohen L F and Jensen H J 1997 *Rep. Prog. Phys.* **60** 1581
[5] Angell C A 1995 *Science* **267** 1924
Ediger M D, Angell C A and Nagel S R 1996 *J. Phys. Chem.* **100** 13200
[6] Bouchaud J P, Cugliandolo L F, Kurchan J and Mezard M 1997 *Spin Glasses and Random Fields* ed A P Young (Singapore: World Scientific)
[7] Vinokur V M, Marchetti M C and Chen L-W 1996 *Phys. Rev. Lett.* **77** 1845
[8] Le Doussal P, Cugliandolo L F and Peliti L 19997 *Europhys. Lett.* **39** 111
[9] Fisher D S, Le Doussal P and Monthus C 1998 *Phys. Rev. Lett.* **80** 3539
[10] Fisher M P A 1989 *Phys. Rev. Lett.* **62** 1415
Fisher D S, Fisher M P A and Huse D A 1991 *Phys. Rev.* B **43** 130
[11] Nattermann T 1990 *Phys. Rev. Lett.* **64** 2454
[12] Nelson D R and Vinokur V M 1992 *Phys. Rev. Lett.* **68** 2398
[13] Giamarchi T and Le Doussal 1994 *Phys. Rev. Lett.* **72** 1530
[14] Nicodemi M and Jensen H J 2001 *J. Phys. A: Math. Gen.* **34** L11
Nicodemi M and Jensen H J 2001 *Phys. Rev. Lett.* **86** 4378
Jensen H J and Nicodemi M 2001 *Europhys. Lett.* **54** 566
[15] Barford W 1997 *Phys. Rev.* B **56** 425
[16] Bassler K E and Paczuski M 1998 *Phys. Rev. Lett.* **81** 3761
Bassler K E, Paczuski M and Altshuler E 2000 *Preprint* cond-mat/0009278
[17] Jensen H J, Brass A and Berlinsky A J 1988 *Phys. Rev. Lett.* **60** 1676
Jensen H J, Brass A, Brechet Y and Berlinsky A J 1990 *Phys. Rev.* B **41** 6394
[18] Nori F 1996 *Science* **271** 1373
Pla O and Nori F 1991 *Phys. Rev. Lett.* **67** 919
Olson C J, Reichhardt C and Nori F 1997 *Phys. Rev.* B **56** 6175
Olson C J, Reichhardt C and Nori F 1998 *Phys. Rev. Lett.* **80** 2197
Olson C J, Reichhardt C and Nori F 1998 *Phys. Rev. Lett.* **81** 3757

[19] Kolton A B, Dominguez D and Grönbech-Jensen N 1999 *Phys. Rev. Lett.* **80** 3061
[20] Reichhardt C, van Otterlo A and Zimanyi G T 2000 *Phys. Rev. Lett.* **84** 1994
Olson C J, Zimanyi G T, Kolton A B and Grönbech-Jensen N 2000 *Phys. Rev. Lett.* **85** 5416
Olson C J, Reichhardt C, Scalettar R T, Zimanyi G T and Grönbech-Jensen N 2000 *Preprint* cond-mat/0006172
Olson C J, Reichhardt C, Scalettar R T, Zimanyi G T and Grönbech-Jensen N 2000 *Preprint* cond-mat/0008350
[21] Giura M, Marcon R, Silva E and Fastampa R 1992 *Phys. Rev.* B **46** 5753
Sarti S, Fastampa R, Giura M, Silva E and Marcon R 1995 *Phys. Rev.* B **52** 3734
[22] Jensen H J 1990 *Phys. Rev. Lett.* **64** 3103
[23] Rudd R E and Broughton J Q 1998 *Phys. Rev.* B **58** R5893
Kohlhoff S, Gumbsch P and Fischmeister H F 1991 *Phil. Mag.* A **64** 851
Bashkirov A G and Zubarev D N 1969 *Theor. Math. Phys.* **1** 311
[24] Binder K 1997 *Rep. Prog. Phys.* **60** 487
[25] Katz S, Lebowitz J L and Spohn H 1983 *Phys. Rev.* B **28** 1655
Schmittmann B and Zia R K P 1995 *Phase Transition and Critical Phenomena* vol 17, ed C Domb and J L Lebowitz (London: Academic)
[26] Hyman R A, Wallin M, Fisher M P A, Girvin S M and Young A P 1995 *Phys. Rev.* B **51** 15304
[27] Nattermann T 1998 *Spin Glasses and Random Fields* ed P Young (Singapore: World Scientific)
[28] Daeumling M, Seuntjens J M and Larbalestier D C 1990 *Nature* **346** 332
Chikumoto N *et al* 1992 *Phys. Rev. Lett.* **69** 1260
Yang G *et al* 1993 *Phys. Rev.* B **48** 4054
Yeshurun Y *et al* 1994 *Phys. Rev.* B **49** 1548
Cai X Y *et al* 1994 *Phys. Rev.* B **50** 16774
Zhukov A A *et al* 1995 *Phys. Rev.* B **51** 12704
Pradhan A K *et al* 1996 *Physica* C **264** 109
Kupfer H *et al* 1996 *Phys. Rev.* B **54** 644
[29] Ghosh K *et al* 1996 *Phys. Rev. Lett.* **76** 4600
Banerjee S S *et al* 1999 *Phys. Rev.* B **59** 6043
[30] Khaykovich B *et al* 1996 *Phys. Rev. Lett.* **76** 2555
Nishizaki T, Naito T and Kobayashi N 1998 *Phys. Rev.* B **58** 11169
Deligiannis K *et al* 1997 *Phys. Rev. Lett.* **79** 2121
[31] Giller D *et al* 1997 *Phys. Rev. Lett.* **79** 2542
Giller D, Shaulov A, Yeshurun Y and Giapintzakis J 1999 *Phys. Rev.* B **60** 106
Baziljevich M *et al* 2000 *Phys. Rev.* B **62** 4058
[32] Radzyner Y *et al* 2000 *Phys. Rev.* B **61** 14362
[33] Cohen L F *et al* 1994 *Physica* C **230** 1
Perkins G K *et al* 1995 *Phys. Rev.* B **51** 8513
[34] Roy S B and Chaddah P 1997 *J. Phys.: Condens. Matter* **9** L625
Ravikumar G *et al* 1998 *Phys. Rev.* B **57** R11069
[35] Kokkaliaris S *et al* 1999 *Phys. Rev. Lett.* **82** 5116
[36] Paltiel Y *et al* 2000 *Nature* **403** 398
[37] Valenzuela S O and Bekeris V 2000 *Phys. Rev. Lett.* **84** 4200
[38] Calame M, Korshunov S E, Leemann Ch and Martinoli P 2001 *Phys. Rev. Lett.* **86** 3630
(Calame M, Korshunov S E, Leemann Ch and Martinoli P 2000 *Preprint* cond-mat/0009308)
[39] van der Beek C J, Colson S, Indenbom M V and Konczykowski M 2000 *Phys. Rev. Lett.* **84** 4196
Giller D, Shaulov A, Tamegai T and Yeshurun Y 2000 *Phys. Rev. Lett.* **84** 3698
[40] Goffman M F, Herbsommer J A, de la Cruz F, Li T W and Kes P H 1998 *Phys. Rev.* B **57** 3663
Correa V F, Nieva G and de la Cruz F 1999 *Phys. Rev. Lett.* **83** 5322
[41] Coniglio A and Nicodemi M 1999 *Phys. Rev.* E **59** 2812
[42] Papadopoulou E L, Nordblad P, Svedlindh P, Schöneberger R and Gross R 1999 *Phys. Rev. Lett.* **82** 173
[43] Niderost M, Suter A, Visani P and Mota A C 1996 *Phys. Rev.* B **53** 9286
Amann A, Mota A C, Maple M B and Löhneysen H V 1998 *Phys. Rev.* B **57** 3640
[44] Fuchs D T *et al* 1998 *Phys. Rev. Lett.* **80** 4971
[45] Marchevsky M, Higgins M J and Bhattacharya S 2001 *Nature* **409** 591
[46] Gurevich A and Vinokur V M 1999 *Phys. Rev. Lett.* **83** 3037
[47] Troyanovski A M, Aarts J and Kes P H 1999 *Nature* **399** 665
[48] Monier D and Fructer L 2000 *Eur. Phys. J.* B **17** 201
[49] Mota A C *et al* 1991 *Physica* C **185–189** 343
Fruchter L *et al* 1991 *Phys. Rev.* B **43** 8709

Stein T *et al* 1999 *Phys. Rev. Lett.* **82** 2955
[50] Aupke K *et al* 1993 *Physica* C **209** 255
[51] Mota A C *et al* 1992 *Phys. Scr.* T **45** 69
[52] Mota A C *et al* 1990 *Physica* A **168** 298
Pollini A *et al* 1990 *Physica* B **165–166** 365
Pollini A *et al* 1993 *J. Low Temp. Phys.* **90** 255
[53] Hoekstra A F Th 1998 *Phys. Rev. Lett.* **80** 4293
[54] Nicodemi M and Coniglio A 1997 *J. Phys. A: Math. Gen.* **30** L187
Coniglio A, de Candia A, Fierro A and Nicodemi M 1999 *J. Phys. C: Solid State Phys.* A **11** 167
[55] Kwok W K *et al* 1994 *Phys. Rev. Lett.* **72** 1092
[56] Safar H *et al* 1995 *Phys. Rev.* B **52** 6211
[57] Bhattacharya S and Higgins M J 1993 *Phys. Rev. Lett.* **70** 2617
Bhattacharya S and Higgins M J 1995 *Phys. Rev.* B **52** 64
Henderson W, Andrei E Y, Higgins M J and Bhattacharya S 1996 *Phys. Rev. Lett.* **77** 2077
Henderson W, Andrei E Y and Higgins M J 1998 *Phys. Rev. Lett.* **81** 2352
[58] Xiao Z L, Andrei E Y and Higgins M J 1999 *Phys. Rev. Lett.* **83** 1664
Xiao Z L, Andrei E Y, Shuk P and Greenblatt M 2000 *Phys. Rev. Lett.* **85** 3265
[59] Nicodemi M and Coniglio A 1999 *Phys. Rev. Lett.* **82** 961
Nicodemi M and Coniglio A 2000 *J. Phys. C: Solid State Phys.* **12** 6601
Nicodemi M 1999 *Phys. Rev. Lett.* **82** 3734
[60] Lefloch F, Hamman J, Ocio M and Vincent E 1992 *Europhys. Lett.* **18** 647
Jonason K, Vincent E, Hamman J, Bouchaud J P and Nordblad P 1998 *Phys. Rev. Lett.* **81** 3243
Alberici-Kious F, Bouchaud J P, Cugliandolo L F, Doussineau P and Levelut A 1998 *Phys. Rev. Lett.* **81** 4987
[61] Fisher D S and Huse D A 1988 *Phys. Rev.* B **38** 373
Bray A J and Moore M A 1987 *Phys. Rev. Lett.* **58** 57
[62] D'Anna G *et al* 1995 *Phys. Rev. Lett.* **75** 3521
[63] Koshelev A E and Vinokur V M 1994 *Phys. Rev. Lett.* **73** 3580
Balents L and Fisher M P A 1995 *Phys. Rev. Lett.* **75** 4270
Giamarchi T and Le Doussal P 1996 *Phys. Rev. Lett.* **76** 3408